Journal of Immunological Methods 364 (2011) 40–49

Contents lists available at ScienceDirect

Journal of Immunological Methods

journal homepage: www.elsevier.com/locate/jim

Research paper

Module based antibody engineering: A novel synthetic REDantibody

Anatoliy Markiv [a], Bernard Anani [a], Ravi V. Durvasula [b], Angray S. Kang [a,*]

[a] Department of Molecular and Applied Biosciences, School of Life Sciences, University of Westminster, 115 New Cavendish Street, London, W1W 6UW, UK
[b] Department of Internal Medicine, School of Medicine and VA Health Care System, University of New Mexico, 1501 San Pedro Ave SE, Albuquerque, NM 87108, USA

ARTICLE INFO

Article history:
Received 18 May 2010
Received in revised form 25 October 2010
Accepted 26 October 2010
Available online 3 November 2010

Keywords:
Antibody engineering
Fluorescent proteins
scFv
Synthetic antibody

ABSTRACT

We describe the facile generation of a stable recombinant antibody with intrinsic red fluorescent properties for qualitative and potentially quantitative immunofluorescence analysis. The REDantibody based on the X-ray crystallographic structures of the anti-sialyl-Tn antibody B72.3 and 3D model of the monomeric red fluorescent protein was designed to retain optimal spatial geometry between the C- and N-termini of the V_H and V_L chains respectively to mimic the domains interface pairing in antibody Fab fragments and to incorporate the red fluorescent protein as a bridging scaffold. The model was further validated by assembling a REDantibody based on CA19.9 the anti-sialylated Lewis (Le)[a] blood group antigen and 4D5-8 the anti-$p185^{HER2}$ antibodies. The chimeric heavy and light chains containing red fluorescent protein as a bridge were correctly processed and secreted into *Escherichia coli* periplasm for assembly and disulphide bond formation, further analysis revealed the molecules to be exclusively monomers. Purified anti-glycan proteins were used for an immunofluorescent analysis of *Trypanosoma cruzi* epimastigotes, and the anti-$p185^{HER2}$ used to determine the binding properties. The REDantibody platform facilitates rapid generation of scFv chimeras that could be used for screening antibodies against cell surface markers. Furthermore, such modular assembly should permit the interchange of binding sites and of fluorophores to create robust panels of coloured antibodies.

1. Introduction

The development and application of optical techniques to visualise the genetically encoded fluorescent proteins (FPs) in living systems has been recognised as an important tool for studies of cell biology and physiology. To allow multiplexing in these studies a palette of FPs has been created that span the visible spectrum from deep blue to near infrared (Tsien, 2009). In parallel the advances in antibody engineering technology have generated a plethora of recombinant antibodies against a diverse range of targets (Winter and Milstein, 1991; Winter, 1998; Lerner, 2006). Although these two genetically encoded molecules would appear to readily permit further modular combinatorial expansion as fusions to produce bifunctional molecules with combined binding and fluorescent properties, such as single chain fragment variable (scFv) regions fused directly to a fluorescent protein either at the C- or N-termini (Griep et al., 1999; Bazl et al., 2007; Olichon and Surrey, 2007; Serebrovskaya et al., 2009), the uptake and application of scFv–fluorophore fusions has been limited. The FPs have in common a very rigid β-barrel structure that can withstand fusions to either the N- or C-termini (Hink et al., 2000) and extensive permutations to two of the exposed loops without impacting on the optical fluorescence properties (Pavoor et al., 2009). On the other hand the scFv's stability is not as robust and varies on a case by case basis, in some instances may be prone to aggregation, thus present stability issues. To date many antibody structures have been determined by X-ray crystallography and the distance between the C-terminal on the variable heavy chain and the N-terminal on the variable light chain has been determined to be approximately 34–35 Å (Arndt et al., 1998).

* Corresponding author. Tel.: +44 2079115000x3556; fax: +44 2079115087.
E-mail address: kanga@wmin.ac.uk (A.S. Kang).

0022-1759/$ – see front matter © 2010 Elsevier B.V. All rights reserved.
doi:10.1016/j.jim.2010.10.009

To generate conventional scFv antibodies a 20–30 amino acid flexible linker is inserted between these two termini which can span more than 35 Å (Bird et al., 1988; Huston et al., 1988). This is important because the non-covalent interactions between variable heavy and light (V_H/V_L) interfaces are critical for antigen recognition. Nevertheless, in scFv's with such long flexible linkers the V_H/V_L pairing exists in equilibrium with the unpaired state, often resulting in aggregation, reduced efficacy and decreased stability relative to the Fab fragment or whole IgG, where the dissociation is restricted. This may be addressed by engineering the V_H and V_L interface residues to enhance association and thus stability (Worn and Pluckthun, 2001), but this would need to be done on a cases by case for each scFv. However, alternatively linking the V_H and V_L via a correctly folded rigid β-barrel structure such as a monomeric FP could provide a generic solution to facilitate optimal interface pairing. Using such a rigid linker would favour V_H/V_L orientation, association and restrict dissociation, ensure monomeric assembly, thus potentially confer Fab-like stability at the same time introducing the fluorophore properties. In essence replacing the C_{H1} and C_L domains of Fab with a single FP domain.

Here we report the design, assembly, production and characterisation of a V_H–RFP–V_L–His-tag (REDantibody) molecule, where monomeric red fluorescent protein (mRFP) from *Discosoma* (Campbell et al., 2002) is inserted as a rigid linker between the V_H and V_L domains of three recombinant distinct antibodies, anti-carbohydrate antibodies B72.3 (Brady et al., 1991), CA19.9 (Koprowski et al., 1979) and 4D5-8 anti-$p185^{HER2}$ (Eigenbrot et al., 1993). The resulting recombinant molecules are characterised by SDS–PAGE, size exclusion chromatography, spectrophotometry, surface plasmon resonance and by utility in immunofluorescence detection of *Trypanosoma cruzi* epimastigotes by confocal microscopy to demonstrate that the two functionalities are retained, i.e., binding affinity and optical properties.

2. Materials and methods

2.1. Molecular design and visualisation

Structure of B72.3 and 4D5-8 antibodies were downloaded from PDB database (PBD: 1BBJ and 1FVC respectively). RFP structure was predicted using Swiss-Model Workspace server. Further modelling was performed using MIFit+ software version 2009.09-1 (Rigaku) and protein models were viewed using PyMol software version 1.1 (DeLano Scientific).

2.2. Plasmids, primers and synthetic DNA

Plasmid pBAK1, previously constructed in our laboratory, is based on pET-26b vector (Novagen). All primers were purchased from Invitrogen. Synthetic DNA sequences of B72.3 and CA19.9 antibody variable domains in V_H–V_L orientation were codon optimised for *Escherichia coli* (*E. coli*) expression and purchased from Epoch Biolabs as plasmids pBSK-B72.3 and pBSK-CA19.9 respectively, with *Nco*I, *Bam*HI and *Not*I restriction sites to facilitate construction of the expression vectors. Plasmid pAK19 encoding the 4D5-8 V_H and V_L was provided by Dan Yansura (Genentech, USA). Plasmid pMT-RFP with mRFP1 gene was a gift from Professor Ray St. Ledger (University of Maryland, USA).

2.3. Bacterial strains, growth media and recombinant DNA technique

XL1-Blue *E. coli* strain (Stratagene) was used for plasmid construction steps. To express recombinant antibodies BL21 (DE3) strain of *E. coli* (Novagen) was used. *E. coli* cells were grown in Lysogeny Broth (LB) (Bertani, 2004) or LB agar plates. Kanamycin sulfate and carbenicillin were used at 30 μg/mL and 100 μg/mL final concentrations respectively. Plasmid DNA was isolated using QIAprep Spin Miniprep Kit (Qiagen) and DNA from the gel was purified using QIAquick Gel Extraction Kit (Qiagen). The *E. coli* cells were transformed using standard heat shock methods. Restriction and modification enzymes were purchased from New England Biolabs (NEB). Final plasmid constructs were confirmed by DNA sequence analysis.

2.4. Construction of the expression plasmid

Antibody scFv encoding fragments were either digested directly from pBSK-B72.3, pBSK-CA19.9 or assembled from V_H and V_L domains encoded by pASK19 plasmids respectively and inserted into *Nco*I and *Not*I restriction sites of previously digested plasmid pBAK1 to make pBAK1B72.3, pBAK1CA19.9 and pBAK14D5-8 respectively. The competent *E. coli* XL1 Blue cells were transformed using ligation mixtures and the clones were selected on the LB plates containing kanamycin. Positive clones were confirmed by DNA sequencing. To make RFP chimeras in V_H–RFP–V_L orientation, plasmids pBAK1B72.3, pBAK1CA19.9 and pBAK14D5-8 were digested with *Bam*HI restriction enzyme and PCR product of mRFP1 gene obtained using pMT-RFP plasmid template and oligonucleotide primers RFPBamHIF and RFPBamHIR (Table 1), inserted to produce pBAK1B72.3RFP, pBAK1CA19.9RFP and pBAK14D5-8RFP respectively. Colonies were initially screened by colony PCR using primers T7F and RFPBamHIR (Table 1) and selected clones confirmed by plasmid DNA sequencing.

2.5. Antibody expression in E. coli

To express scFv and REDantibody chimeras, *E. coli* BL21 (DE3) (Novagen) cells were transformed with the appropriate plasmid and plated onto LB agar supplemented with kanamycin sulfate (30 μg/mL final concentration). The cells were allowed to grow at 37 °C for 18 h and the following day, five fresh colonies were inoculated into 10 mL of LB media (with antibiotics) and grown at 37 °C (with shaking at 250 rpm) for 16 h. Next day, 200 mL of pre-warmed LB media, prepared in 1 L conical flasks (with antibiotics), was inoculated with 10 mL of the overnight culture and grown at 37 °C (with shaking at 250 rpm) until the optical density at 600 nm had reached 0.5, then the cells were placed on ice for 30 min and Isopropyl β-D-1-thiogalactopyranoside (IPTG) added (final concentration 0.3 mM) to the cultures and the cells were grown at 20 °C for an additional 20 h with shaking at 250 rpm. Bacterial cells were pelleted by centrifugation for 20 min, 5000 rpm at 4 °C (using Sorvall SuperT 21 bench top

Table 1
PCR primers used in REDantibody assembly.

Name	Oligonucleotide sequence	Cloning site
RFPBamHIF	CAGT**GGATCC**GAGGACGTCATCAAGGAGTTC	*Bam*HI
RFPBamHIR	CAGT**GGATCC**GCCTCCGCCTGTGCGGCCCTCGGCGCGCTCGTAC	*Bam*HI
T7F	GCAGCTAATACGACTCACTATAGG	

centrifuge, with SL-250 T rotor), the supernatant discarded and the pellets retained for periplasmic protein extraction.

2.6. Antibody purification from E. coli periplasm

Bacterial cell pellets from 200 mL culture were resuspended in 10 mL of periplasmic buffer (30 mM Tris–base, pH 8.0, 20% sucrose and 1 mM EDTA) supplemented to a final concentration of 0.1 mM phenylmethylsulfonyl fluoride (PMSF). The cells were incubated on ice for 10 min and centrifuged at 9000 rpm for 10 min at 4 °C (using Sorvall SuperT 21 bench top centrifuge, with SL-50 T rotor). The supernatants were collected and stored on ice, while cell pellets were resuspended in 7 mL of 5 mM $MgCl_2$ (4 °C). After incubation for 5 min on ice, bacterial cells were pelleted by centrifugation as described before, and the supernatants combined to give the periplasmic fraction.

2.7. Ni-NTA purification of recombinant proteins

Recombinant proteins were purified using a 1-mL HisTrap HP column (GE Healthcare) fitted to an ÄKTAprime™ plus (GE Healthcare) liquid chromatography system. First, the 1-mL column was equilibrated with 5 column volumes of equilibration buffer (20 mM Tris–HCl, pH 8.0, 500 mM NaCl, 10 mM imidazole). Following this, 17 mL *E. coli* periplasmic fraction (diluted two times with 20 mM Tris–HCl, pH 8.0, 500 mM NaCl buffer) was loaded onto the column and the column was washed with 5 column volumes of wash buffer (20 mM Tris–HCl, pH 8.0, 500 mM NaCl, 20 mM imidazole). The protein was eluted with 5 column volumes of elution buffer (20 mM Tris–HCl, pH 8.0, 500 mM NaCl, 500 mM imidazole) and collected in 1 mL aliquots. Protein elution was monitored at 280 nm. Eluted fractions 1–5 were analysed by SDS–PAGE.

2.8. Desalting and anion exchange chromatography

Recombinant antibody obtained by Ni-NTA purification was desalted using 40 mL Sephadex G25 column (GE Healthcare) fitted to an ÄKTAprime™ plus (GE Healthcare) liquid chromatography system in 20 mM Tris–HCl, pH 8.0 buffer and further purified using 1 mL HiTrap Q Sepharose FF column (GE Healthcare) and eluted by increasing buffer salt concentration. First, a 1-mL column was equilibrated with 5 column volumes of equilibration buffer (20 mM Tris–HCl, pH 8.0). Following this, 5 mL of desalted antibody fraction was loaded onto the column and protein was eluted by increasing concentration of NaCl in 20 mM Tris–HCl, pH 8.0 buffer and collected into 1-mL fractions. Eluted antibodies were concentrated and the buffer exhanged to 20 mM Tris–HCl, pH 8.0 and 150 mM NaCl using Ultracel YM-10 Amicon centrifugal devices from Millipore. Protein concentration was determined using Bradford assay kit (Bio-Rad) (Bradford, 1976).

2.9. Size Exclusion Chromatography

SEC was performed on an ÄKTAprime™ plus using a HiLoad 16/60 Superdex 200 size-exclusion column (GE Healthcare, Amersham, UK) equilibrated with degassed phosphate buffered saline (PBS). The purified proteins were separated by loading 1 mL of the sample at a concentration of 100–200 μg/mL. The flow rate was 1 mL/min, and the absorbance of the eluted protein was monitored at 280 nm. The column was calibrated with the following protein standards: β-amylase (200 kDa), bovine serum albumin (66 kDa), carbonic anhydrase (29 kDa) and cytochrome *c* (12.4 kDa).

2.10. SDS–PAGE

The fractions eluted from the HisTrap column (1–5) were analysed by SDS–PAGE using 12% Tris–glycine gels. Proteins were stained with Coomassie Blue R250 as follows: after electrophoresis gel was submerged in plastic container into 50 mL of 0.025% Coomassie Blue in 10% acetic acid solution and heated in the microwave until boiling (approximately 1 min), cooled down for 2 min on bench and destained in 50 mL of 10% acetic acid by repeating previous procedure of heating in microwave and cooling down. Finally, the gel was kept in 10% acetic acid before scanning.

2.11. Optical properties determination

The fluorescent measurements were carried out using SpectraMAX Gemini EM fluorescence microplate reader with Gemini EM software (Molecular Devices, UK) using Optiplex 96 F microtitre plates (Perkin Elmer, UK) with REDantibody 4D5-8, 50 μg in 0.1 mL/well in phosphate-buffered saline (137 mM NaCl, 2.5 mM KCl, 10 mM Na_2HPO_4 and 1.8 mM KH_2PO_4) pH 7.4. Excitation and emission spectra between 500 and 650 nm were determined at 2-nm intervals and the arbitrary fluorescence units (AFU) recorded. The concentration-dependent fluorescence with excitation 584 nm and emission 607 nm was determined for tenfold serial dilutions of REDantibody 4D5-8 from a stock solution of 95 nmol.

2.12. Surface plasmon resonance (SPR) measurements

The SPR measurements were carried out on the BIAcore 3000 following the procedure previously described to determine the binding of 4D5-8 scFv with $p185^{HER2\text{-}ECD}$ (Worn and Pluckthun, 1998).The $p185^{HER2\text{-}ECD}$ antigen (Sino Biological Inc, Beijing, China) 100 μg/mL in 20 mM citrate buffer pH 4.0 was coupled to the CM-5 research grade sensor chip using an amine coupling kit (GE Healthcare). The 4D5-

8 REDantibody were applied at 50, 100, 175, 250 and 500 μg/mL to the chip at a flow rate of 20 μl/min at 20 °C. The surface was regenerated by injection of 45 μl of 0.1 M glycine–HCL, pH 2.2, 0.5 M NaCl. Data were analysed using the global fit in the BIAevaluation program version 4.1.

2.13. Immunofluorescent confocal microscopy

Wild-type *T. cruzi* epimastigote 4-day-old cultures were fixed with 2% paraformaldehyde in phosphate buffer and allowed to adhere onto glass slides. Adhered cells were washed with PBS and non-specific antigen-binding sites were blocked with 2% BSA in PBS, pH 8.0, for 1 h at room temperature. Samples were incubated for 60 min at room temperature with recombinant REDantibodies. REDantibody 4D5-8 was used as a negative control. Slides were mounted in *N*-propylgalate (Sigma P130) to reduce photobleaching and observed on a Leica SP2 Confocal Laser Scanning Microscope, using 543-nm He-Ne laser. All images were analysed using IMARIS software version 6.3 (Bitplane). Formaldehyde fixed *T. cruzi* epimastigotes TC1 strain were a gift from Professor Michael Miles and Michael Lewis.

3. Results

3.1. Molecular design

The X-ray crystallographic structure of Fab B72.3 (PDB: 1BBJ) reveals that the distance between the C-terminal Ser114 on the variable heavy chain and the N-terminal Asp1 on the variable light chain is approximately 34 Å. A search of the Protein Data Base (PDB) was carried out to identify structures with N- and C-termini protruding from the same plane with spacing of 20–30 Å apart without intersecting the rest of the protein. Fortuitously, mRFP1 met these criteria with the distance between Val7 and His221 of the termini in fast maturing red fluorescent protein DsRed variant (PDB 2VAE) being approximately 25 Å. Direct fusion of the V_H to the N-terminus and V_L to the C-terminus would have resulted in a linkage 9 Å shorter than the optimal spacing revealed by X-ray crystallographic structure of B72.3. This was overcome by modelling the N- and C-termini to include Gly_4Ser linkers on each end of RFP (Fig. 1). The resulting model could accommodate the variable regions of the antibody with a molecular geometry approaching that determined from the X-ray studies.

3.2. DNA manipulation

The REDantibody constructs were assembled in a modified pET-26b vector (Novagen) with a *pel*B leader sequence to direct secretion to the periplasm of *E. coli* (Fig. 2A). The synthetic genes of the V_H–V_L scFv antibodies were designed to encode an in-frame *Bam*HI site between the V_H and V_L regions and the whole flanked by *Nco*I and *Not*I sites for in-frame directional cloning. The mRFP gene was inserted into each of these plasmids to make expression plasmids pBAK1B72.3RFP and pBAK1CA19.9RFP as shown in Fig. 2A. The control pBAK14D5-8RFP was assembled in a similar manner after removing an internal *Bam*HI site. The expression cassettes starts from *pel*B leader sequence followed by V_H chain, RFP, V_L chain and an octa-histidine-tag at the carboxyl terminus of the resulting protein sequence as shown in Fig. 2B.

3.3. Protein expression and purification

The recombinant scFv and the corresponding REDantibody proteins were expressed in BL 21 (DE3) *E. coli* strain and recovered from the periplasmic extract and purified via Ni-NTA affinity chromatography. Protein expression and purification processes were monitored by SDS–PAGE. The protein concentration of the recovered functional protein was determined for each construct; mRFP (20 mg/L), REDantibody 4D5-8 (5 mg/L),

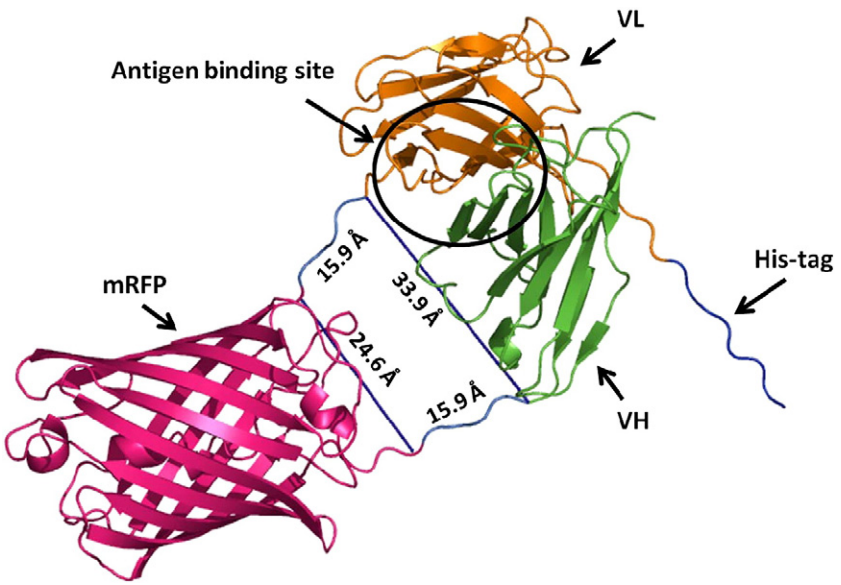

Fig. 1. Ribbon representation of a REDantibody molecule 3D model. VH chain is shown in green, RFP domain in red, VL chain in yellow. His-tag is shown in blue and linkers between V_H–RFP and RFP–VL are in cyan with the distances indicated. Antigen binding site is indicated as a black circle on antibody structure. All distances are indicated in angstroms (Å).

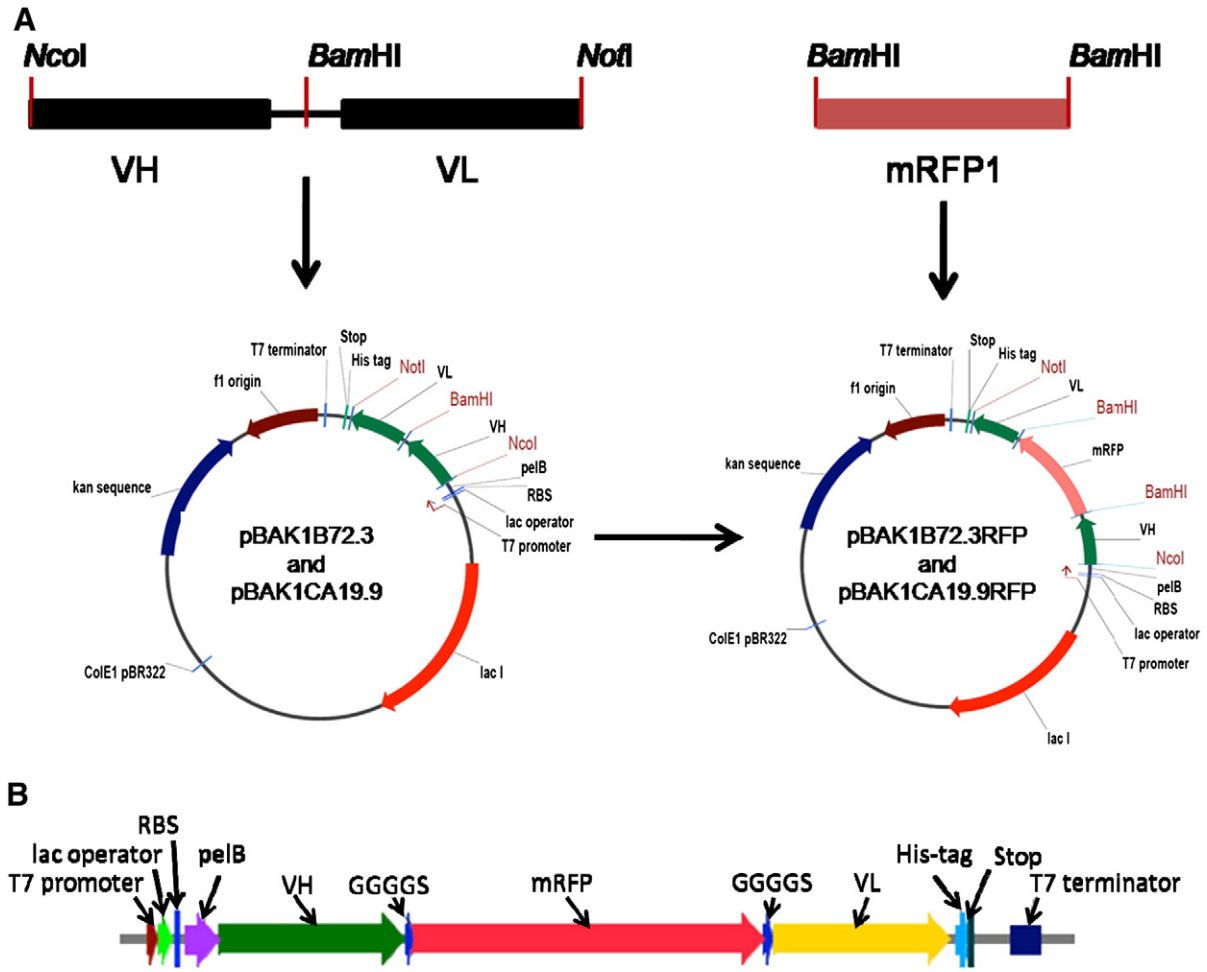

Fig. 2. Generation of expression plasmid (A) and *E. coli* expression cassette (B) of REDantibody. (A) The single chain Fv encoding fragment flanked by *Nco*I and *Not*I sites with an in-frame *Bam*HI site between the VH and VL was inserted into pBAK1 vector to generate pBAK1B72.3, pBAK1CA19.9 (and pBAK14D5 not shown). The mRFP encoding fragment flanked by *Bam*HI sites was inserted into the pBAK1B72.3, CA19.9 and 4D5 to generate pBAK172.3RFP, pBAK1CA19.9RFP and pBAK14D5RFP. (B) The expression cassette has a T7 promoter to initiate transcription using T7 RNA polymerase, lac operator is for the control of transcription using IPTG. RBS is ribosome binding site where translation begins, pelB sequence to guide newly synthesised molecule into the *E. coli* periplasm where this sequence is deleted and disulphide bonds are formed. VH is variable heavy chain of antibody, Link is an additional 5 amino acids to the mRFP1 gene, mRFP is a gene of red fluorescent protein and VL is variable light domain of antibody. This is followed by His-tag sequence for immobilised metal affinity purification and stop codon. T7 terminator is to terminate transcription by T7 RNA polymerase.

REDantibody CA19.9 (0.88 mg/L) and REDantibody (72.3 0.9 mg/L). The predicted molecular weights of the scFv and REDantibody recombinant proteins were approximately 25 and 51 kDa respectively as shown in Fig. 3. The SDS–PAGE analysis of the Ni-NTA affinity enriched recombinant antibodies also had other protein bands corresponding to co-enriched *E. coli* host proteins. The size exclusion column was calibrated using a standard range 200–12 kDa (Sigma, UK) prior to use (Fig. 4A). The mRFP protein elution corresponded to monomer of 25 kDa (Fig. 4B). A single REDantibody peak eluted at fractions/time corresponding to ~51 kDa (Fig. 4C). Moreover the colour of REDantibody *E. coli* culture, periplasmic and elution fractions were pink (data not shown).

3.4. Fluorophore measurements

The excitation and emission peaks of REDantibody 4D5-8 were determined to be 584 and 607 nm as shown in Fig. 5A. The concentration-dependent emission at 607 nm permitted accurate detection of 9.5 pmole of this REDantibody as shown in Fig. 5B.

3.5. BIAcore measurements

The association and disassociation rate for REDantibody 4D5-8 binding to $p185^{HER2\text{-}ECD}$ was determined to be $2.19 \times 10^{-4} \pm 0.13 \times 10^{-4}$ $M^{-1}s^{-1}$ and $4.43 \times 10^{-5} \pm 1.04 \times 10^{-5}$ s^{-1} respectively and the K_D calculated to be 2.2 ± 0.8 nM ($n = 3$, data not shown).

3.6. Immunofluorescent staining and confocal microscopy

Functional analysis of the REDantibody was based on well-characterised properties of B72.3 and CA19.9 antibodies to recognise sialyl-Tn and sialylated Lewis (Le)[a] blood group antigen respectively (Reddish et al., 1997; Pant et al., 2008)

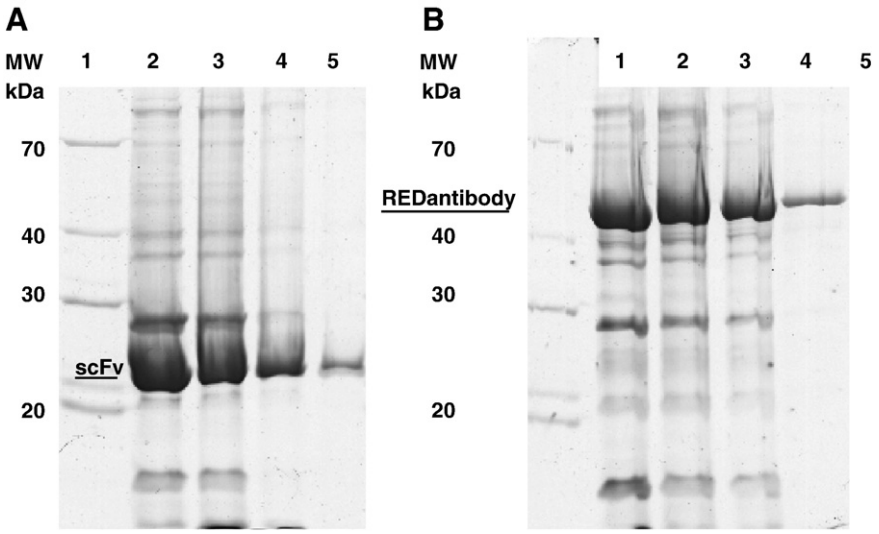

Fig. 3. Expression and purification (A) CA19.9 scFv and (B) CA19.9 REDantibody. The purified scFvCA19.9 (A) and REDantibodyCA19.9 (B) were resolved by 12% SDS–PAGE and stained with Coomassie Brilliant Blue R250. Lane 1: molecular weight markers, 70, 40, 30 and 20 kDa; lane 2: Ni-NTA column elution 1; lane 3: Ni-NTA column elution 2; lane 4: Ni-NTA column elution 3; lane 5: Ni-NTA column elution 4.

which are part of a panel of markers used in cancer diagnostics (Betta et al., 1991). Interestingly the same antigen has been detected on the surface of the human pathogen *T. cruzi* (Freire et al., 2003). The 4D5-8 REDantibody was constructed for use as a negative control since it recognises a peptide epitope on $p185^{HER2}$ and not sialyl glycan. This was confirmed by the fluorescent staining of *T. cruzi* epimastigotes using purified recombinant anti-glycan REDantibodies shown in Figs. 6A and B. The control REDantibody 4D5-8 did not label the parasites (Fig. 6C). The maximum intensity fluorescence

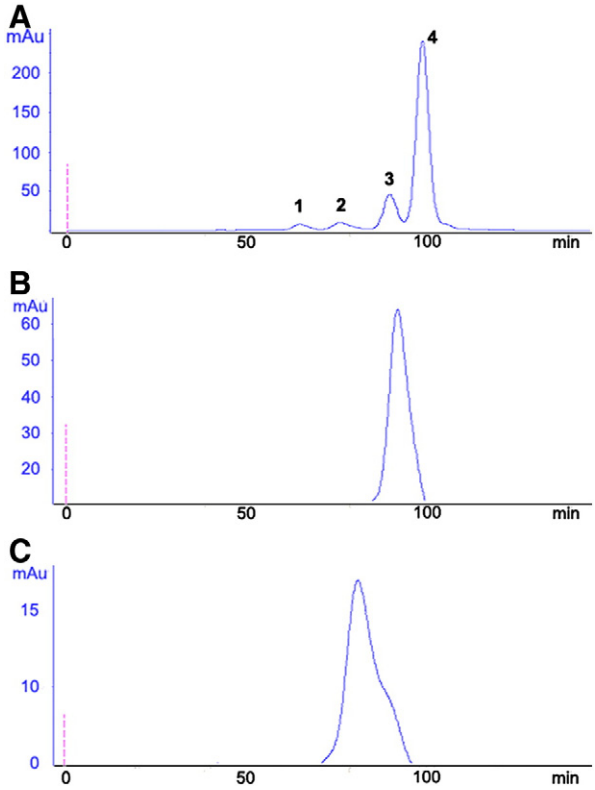

Fig. 4. Gel filtration on Sephadex G200 column. Panel A—standard proteins (peak1—200 kDa, peak 2—66 kDa, peak 3—29 kDa, peak 4—12.4 kDa); Panel B—mRFP1; and panel C—REDantibodyCA19.9.

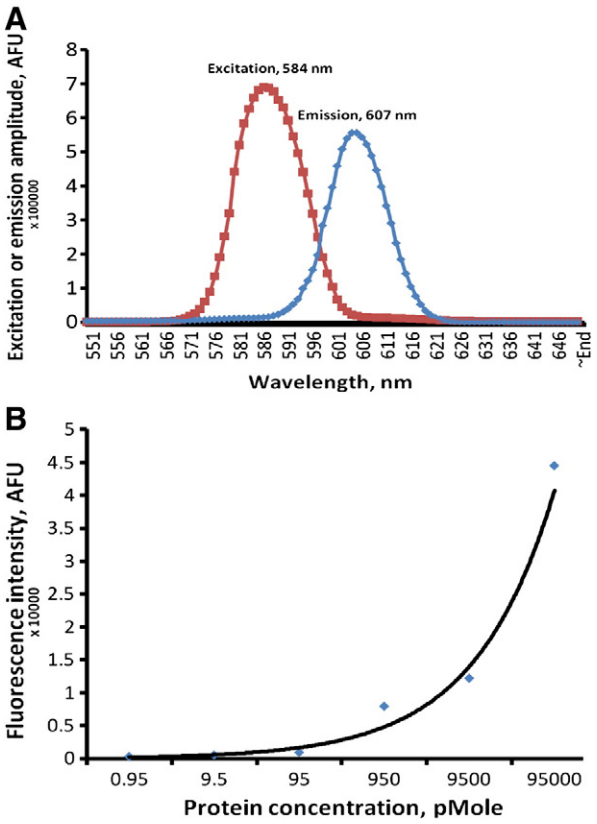

Fig. 5. Spectrophotometric analysis of REDantibody Scanning fluorescent spectrophoptometry of REDantibody 4D5-8 (A) and concentration-dependent fluorescent intensity of REDantibody 4D5-8 (B).

staining image with REDantibody CA19.9 (Fig. 6D) revealed the appearance of a cleft area on the parasite surface with reduced staining. Confocal three-dimensional imaging (Fig. 6E) confirmed the presence of a depression corresponding to the cleft observed earlier.

4. Discussion

Molecules tagged with fluorophores in particular antibodies are highly sensitive tools used in imaging and for cell sorting. Conventional organic fluorophores exemplified by FITC, TRITC, CY-3, and CY-5 are chemically conjugated to the antibodies in vitro. Chemical conjugation is dependent on the availability of particular amino acid side chains. The inappropriate conjugation in or in close proximity of the binding site can reduce the binding efficacy of the parental antibody. The number of labels incorporated into each antibody molecule in the preparation also varies and limits the utility of these reagents in quantitative analysis. The actual chemical link itself may be prone to cleavage over time resulting in leaching of fluorophore. The chemical fluorophores also fade due to photobleaching upon excitation. Also in the case with whole immunoglobulin the binding to Fc receptors presents problems in immunohistochemical analysis. Significant advances have been made in conjugation chemistry to attempt to overcome some of these difficulties with whole antibodies or Fab fragments. With the application of recombinant DNA technology, scFvs have been engineered to incorporate a free cysteine at the C-terminus for specific conjugation chemistry or have been fused directly to fluorescent proteins for prokaryotic (Griep et al., 1999; Casey et al., 2000; Hink et al., 2000; Schwalbach et al., 2000; Morino et al., 2001) or eukaryotic expression (Peipp et al., 2004). However conventional scFv's are not ideally suited for these applications. The scFv's are not as stable as whole antibody or the Fab fragment (Worn and Pluckthun, 2001). In the scFv if the flexible linker that joins the V_H and V_L domains is long (>20 amino acids) it is prone to aggregation since such a long linker permits the dissociation of the V_H and V_L domains. If the linker length is reduced scFv is prone to form a mixture of multimers (dimers, trimers) (Holliger et al., 1993). However the multimeric assemblies may have altered binding kinetics. Fusing a scFv assembled with a long linker directly to GFP would not necessarily reduce the aggregation properties of the scFv. Likewise using a scFv with shorter linkers would favour multimer formation which may or may not retain optimal affinity for the target. Despite these issues the concept of having a genetically encoded affinity label is very appealing since it provides a simple platform for creating uniform diagnostic reagents. An alternative approach to this problem has been to modify an FP to incorporate two extended loops that can form recognition motifs, while retaining the fluorophore properties, although not antibodies as such, they have potential (Pavoor et al., 2009). However the antibody based binding site composed of a V_H and V_L with a total of six loops with an extremely high combinatorially diverse $CDRH_3$ and $CDRL_3$ from natural and synthetic repertoires provide a vast range of high affinity binding sites (Winter, 1998; Lerner, 2006). We sought to combine the best features of both the antibody binding sites and the properties of encoded fluorophores (Tsien, 2009) in a single molecule, by inserting the FP between the V_H and V_L domains to spatially orientate the V_H/V_L interfaces to mimic the pairing observed in Fab structures. Our earlier attempts to construct similar bridged molecules using a related β-barrel structure of green fluorescent protein EGFP (PDB 1GFL) (Yang et al., 1996) resulted in molecules that did not bind to the target antigen. We speculate that since the EGFP could exist as a dimer at higher protein concentrations its assembly could sterically hinder V_H/V_L domain pairing, with or without the introduction of Gly4Ser linkers (data not shown). This obstacle was overcome by using a monomeric fluorescent protein with a β-barrel structure exemplified by mRFP1 (Campbell et al., 2002) as shown in Fig. 1.

The vectors constructed encoding the REDantibodies are based on the pET series (Studier, 1991) as shown in Fig. 2. The use of the T7 promoter and the BL21(DE3) host results in high level of expression of the recombinant protein, the majority of which is retained within the cell cytoplasm despite having a *pelB* leader sequence to direct the polypeptide into the bacterial periplasm. The amount of REDantibody recovered varied for each antibody construct, 4D5-8 had the highest recovery (5 mg/L), whereas the recovery of the corresponding anti-sialyl glycan antibodies were both just below 1 mg/L, both levels are comparable to the recovery of scFv from *E. coli*. It may be the recovery of anti-sialyl glycan REDantibodies was reduced since the secreted, correctly folded and functional REDantibody in both cases bound to sialic acid, which is present on the host

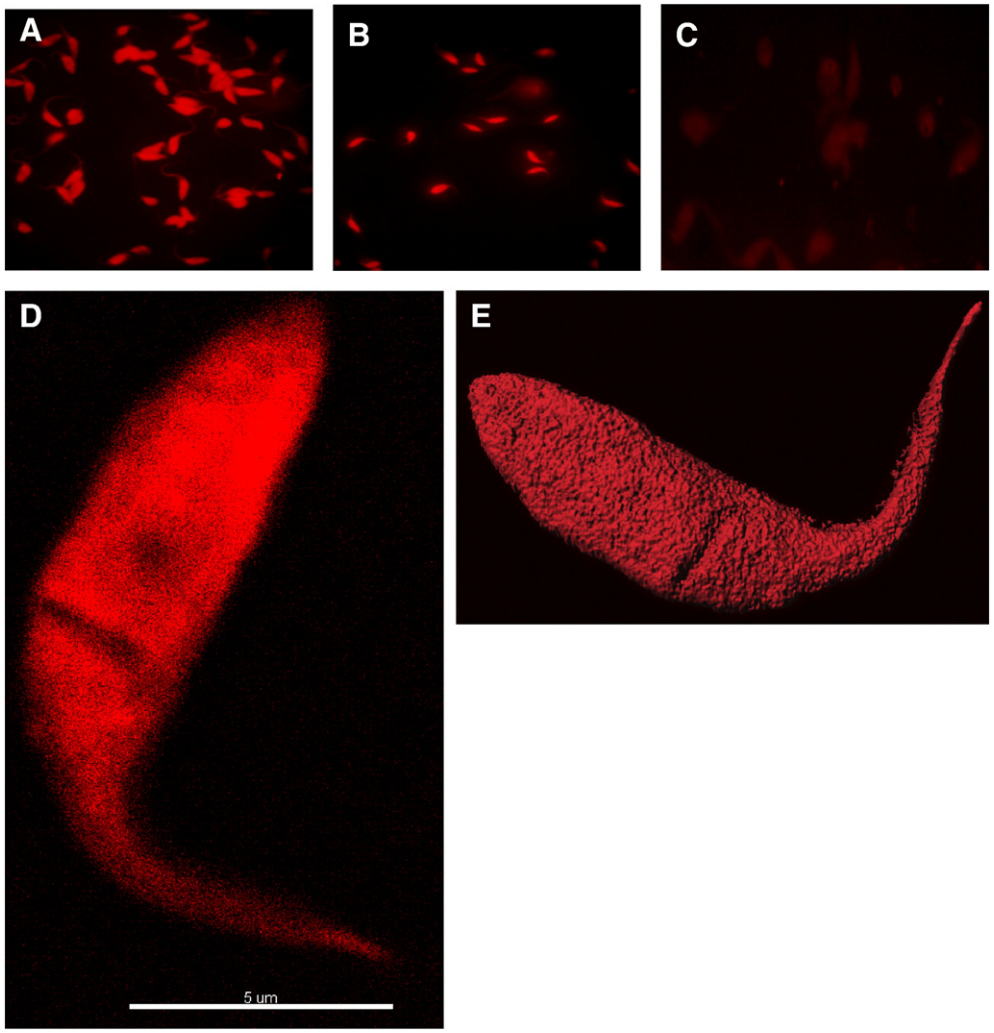

Fig. 6. Immunofluorescent microscopic analysis of *Trypanosoma cruzi* epimastigotes. *T. cruzi* epimastigotes stained with REDantibody. CA19.9 (A), REDantibody B72.3 (B) and negative control REDantibody 4D5-8 (C). *T. cruzi* epimastigote is stained with REDantibody CA19.9 and viewed by microscopy reveals a maximum intensity fluorescent image (D). The surface staining combined with confocal microscopy reveals a slight invagination on the parasite surface (E).

bacterial surface (Barry and Goebel, 1957). Notwithstanding, sufficient REDantibody was recovered from the periplasmic extract to permit further affinity purification and functional analysis. The SDS–PAGE of the affinity isolated CA19.9 scFv and the corresponding REDantibody had polypeptides of 25 and 51 kDa respectively as shown in Fig. 3A and B respectively. Size exclusion chromatography on the affinity purified proteins was used to determine whether the molecules were monomeric or multimeric. The mRFP and REDantibody each eluted with a single peak corresponding to 25 kDa and 51 kDa as shown in Fig. 4 panel B and C respectively, indicating that both proteins are monomers.

A key feature of this REDantibody platform is the intrinsic colour of the bacteria producing the active molecule and of the purified proteins having a visible pink-red colour, thus not necessarily requiring sophisticated detection equipment to follow the purification steps. The excitation and emission wavelengths of REDantibody were determined to be 584 nm and 607 nm respectively (as shown in Fig. 5A) and are identical to that of mRFP (Campbell et al., 2002; Khrameeva et al., 2008), confirming that the fusing immunoglobulin domains to both ends of an FP did not compromise the fluorescent properties. Moreover, it may be possible to detect as little as 9.5 pmol of REDantibody using a standard fluorometer as shown in Fig. 5B. This may permit quantitative analysis of target antigen. The kinetics of binding for the anti-glycan REDantibodies was difficult to perform since a defined antigen preparation was not readily available. Thus we carried out the binding studies on the REDantibody 4D5-8. The calculated K_D value for REDantibody 4D5-8 of 2.19 nM was within the values determined independently for the 4D5-8 scFv with a V_H–$(Gly_4\ Ser)_3$ linker V_L orientation of 194 pM (Worn and Pluckthun, 1998), and 9.4 nM for Herceptin™ (Troise et al., 2008), further confirming that the binding characteristics are not compromised in this format.

The use of this FP would also permit combined use with other conventional dyes for FACs analysis, immunochemistry and confocal microscopy that utilise a range up to 543 nm. In this study we used the REDantibody B72.3 and CA19.9 to visualise the carbohydrate antigens sialyl-Tn and sialylated Lewis (Le)[a] on the surface of *T. cruzi* epimastigotes respectively,

using immunofluorescence (Figs. 6A, B and D) and confocal microscopy (Fig. 6 E). The negative control REDantibody 4D5-8 did not label the parasites when examined using immunofluorescence microscopy implying the specificity was introduced by the antibody binding domains (Fig. 6C). It was observed that the slides prepared for this study could be viewed for at least a week, without noticeable loss of signal implying robust stability of the REDantibody. The mRFP1 derived from DsRed is stable within a wide range of pH 5.0–12.0 and in 6 M urea (Stepanenko et al., 2005); thus, the antibody antigen interaction may be disrupted by adjusting the pH and or the addition of urea and the released fluorophore quantitatively determined in solution. The resulting REDantibody molecule is also stable to photobleaching, thus potentially permitting a higher sensitivity by use of time-resolved pulsed analysis. Another feature of REDantibody is the generation of reactive oxygen species H_2O_2 upon exposure to white light: this may potentially have a wide range of applications in vitro and possibly in vivo, i.e., photo-ablation of target cells (Serebrovskaya et al., 2009). Additionally with a far red emission spectra, these types of targeted molecules may have utility in *in vivo* whole body imaging (Shcherbo et al., 2007). Furthermore, this platform may also be applied to other existing mAbs to create the next generation of diagnostic and cell sorting molecules. The platform may also be used to create libraries of V_H and V_L domains that may be readily accessed using high throughput non-isotopic screening as an alternative phage or other types of display selection technologies. In general the use of other pre-folded protein domains with N- and C-termini in the same spatial plane with spacing close to 20–30 Å may be used in this modular approach to create bifunctional antibodies. The monomeric β-barrel fluorophore architecture used in this study is essentially the same in all the coloured variant (Tsien, 2009), thus enabling the assembly of a palette of genetically encoded antibody based reagents for simultaneous multi-analyte detection.

5. Conclusions

Assembling the REDantibody using the fluorophore as a bridge introduces the following properties: firstly, with an integrated fluorophore, a single reagent has been created, which reduces time, cost and increases reproducibility of the binding assay. Secondly, the antibody binding site and fluorophore are stoichiometric, and thus the signal generated is directly proportional to the amount of antibody bound (i.e., potentially quantitative). Finally, expression and purification steps can be monitored without the need for sophisticated detection equipment since the bacteria and the recombinant protein are visible to the naked eye with a distinct red colour.

6. Funding

This work was supported by the National Institutes of Health [R01 AI066045].

Acknowledgements

We thank Professor Michael Miles for constructive comments, Michael Lewis for providing trypanosomes, Professor Ray St. Ledger for providing the mRFP1 DNA and Dr. Mark JP Kerrigan for assistance with the confocal microscopy. BA is a recipient of a University of Westminster Cavendish Studentship award.

References

Arndt, K.M., Muller, K.M., Pluckthun, A., 1998. Factors influencing the dimer to monomer transition of an antibody single-chain Fv fragment. Biochemistry 37, 12918–12926.
Barry, G.T., Goebel, W.F., 1957. Colominic acid, a substance of bacterial origin related to sialic acid. Nature 179, 206.
Bazl, M.R., Rasaee, M.J., Foruzandeh, M., Rahimpour, A., Kiani, J., Rahbarizadeh, F., Alirezapour, B., Mohammadi, M., 2007. Production of chimeric recombinant single domain antibody-green fluorescent fusion protein in Chinese hamster ovary cells. Hybridoma (Larchmt) 26, 1–9.
Bertani, G., 2004. Lysogeny at mid-twentieth century: P1, P2, and other experimental systems. J. Bacteriol. 186, 595–600.
Betta, P.G., Pavesi, M., Pastormerlo, M., Tallarida, F., Bellingeri, D., Bocca, R., 1991. Use of monoclonal antibody B72.3 as a marker of metastatic carcinoma cells in neoplastic effusions. Pathologica 83, 99–104.
Bird, R.E., Hardman, K.D., Jacobson, J.W., Johnson, S., Kaufman, B.M., Lee, S.M., Lee, T., Pope, S.H., Riordan, G.S., Whitlow, M., 1988. Single-chain antigen-binding proteins. Science 242, 423–426.
Bradford, M.M., 1976. A rapid and sensitive method for the quantitation of microgram quantities of protein utilizing the principle of protein-dye binding. Anal. Biochem. 72, 248–254.
Brady, R.L., Hubbard, R.E., King, D.J., Low, D.C., Roberts, S.M., Todd, R.J., 1991. Crystallization and preliminary X-ray diffraction study of a chimaeric Fab' fragment of antibody binding tumour cells. J. Mol. Biol. 219, 603–604.
Campbell, R.E., Tour, O., Palmer, A.E., Steinbach, P.A., Baird, G.S., Zacharias, D.A., Tsien, R.Y., 2002. A monomeric red fluorescent protein. Proc. Natl Acad. Sci. USA 99, 7877–7882.
Casey, J.L., Coley, A.M., Tilley, L.M., Foley, M., 2000. Green fluorescent antibodies: novel in vitro tools. Protein Eng. 13, 445–452.
Eigenbrot, C., Randal, M., Presta, L., Carter, P., Kossiakoff, A.A., 1993. X-ray structures of the antigen-binding domains from three variants of humanized anti-p185HER2 antibody 4D5 and comparison with molecular modeling. J. Mol. Biol. 229, 969–995.
Freire, T., Robello, C., Soule, S., Ferreira, F., Osinaga, E., 2003. Sialyl-Tn antigen expression and O-linked GalNAc-Thr synthesis by *Trypanosoma cruzi*. Biochem. Biophys. Res. Commun. 312, 1309–1316.
Griep, R.A., van Twisk, C., van der Wolf, J.M., Schots, A., 1999. Fluobodies: green fluorescent single-chain Fv fusion proteins. J. Immunol. Methods 230, 121–130.
Hink, M.A., Griep, R.A., Borst, J.W., van Hoek, A., Eppink, M.H., Schots, A., Visser, A.J., 2000. Structural dynamics of green fluorescent protein alone and fused with a single chain Fv protein. J. Biol. Chem. 275, 17556–17560.
Holliger, P., Prospero, T., Winter, G., 1993. "Diabodies": small bivalent and bispecific antibody fragments. Proc. Natl Acad. Sci. USA 90, 6444–6448.
Huston, J.S., Levinson, D., Mudgett-Hunter, M., Tai, M.S., Novotny, J., Margolies, M.N., Ridge, R.J., Bruccoleri, R.E., Haber, E., Crea, R., et al., 1988. Protein engineering of antibody binding sites: recovery of specific activity in an anti-digoxin single-chain Fv analogue produced in *Escherichia coli*. Proc. Natl Acad. Sci. USA 85, 5879–5883.
Khrameeva, E.E., Drutsa, V.L., Vrzheshch, E.P., Dmitrienko, D.V., Vrzheshch, P.V., 2008. Mutants of monomeric red fluorescent protein mRFP1 at residue 66: structure modeling by molecular dynamics and search for correlations with spectral properties. Biochemistry (Mosc) 73, 1085–1095.
Koprowski, H., Steplewski, Z., Mitchell, K., Herlyn, M., Herlyn, D., Fuhrer, P., 1979. Colorectal carcinoma antigens detected by hybridoma antibodies. Somatic Cell Genet. 5, 957–971.
Lerner, R.A., 2006. Manufacturing immunity to disease in a test tube: the magic bullet realized. Angew. Chem. Int. Ed Engl. 45, 8106–8125.
Morino, K., Katsumi, H., Akahori, Y., Iba, Y., Shinohara, M., Ukai, Y., Kohara, Y., Kurosawa, Y., 2001. Antibody fusions with fluorescent proteins: a versatile reagent for profiling protein expression. J. Immunol. Methods 257, 175–184.
Olichon, A., Surrey, T., 2007. Selection of genetically encoded fluorescent single domain antibodies engineered for efficient expression in *Escherichia coli*. J. Biol. Chem. 282, 36314–36320.
Pant, K.D., Jain, A., McCracken, J.D., Thompson, K., 2008. Immunohistochemical examination of anti-STn monoclonal antibodies LLU9B4, B72.3, and B35.2 for their potential use as tumor markers. Dig. Dis. Sci. 53, 2189–2194.

Pavoor, T.V., Cho, Y.K., Shusta, E.V., 2009. Development of GFP-based biosensors possessing the binding properties of antibodies. Proc. Natl Acad. Sci. USA 106, 11895–11900.

Peipp, M., Saul, D., Barbin, K., Bruenke, J., Zunino, S.J., Niederweis, M., Fey, G.H., 2004. Efficient eukaryotic expression of fluorescent scFv fusion proteins directed against CD antigens for FACS applications. J. Immunol. Methods 285, 265–280.

Reddish, M.A., Jackson, L., Koganty, R.R., Qiu, D., Hong, W., Longenecker, B.M., 1997. Specificities of anti-sialyl-Tn and anti-Tn monoclonal antibodies generated using novel clustered synthetic glycopeptide epitopes. Glycoconj. J. 14, 549–560.

Schwalbach, G., Sibler, A.P., Choulier, L., Deryckere, F., Weiss, E., 2000. Production of fluorescent single-chain antibody fragments in *Escherichia coli*. Protein Expr. Purif. 18, 121–132.

Serebrovskaya, E.O., Edelweiss, E.F., Stremovskiy, O.A., Lukyanov, K.A., Chudakov, D.M., Deyev, S.M., 2009. Targeting cancer cells by using an antireceptor antibody-photosensitizer fusion protein. Proc. Natl Acad. Sci. USA 106, 9221–9225.

Shcherbo, D., Merzlyak, E.M., Chepurnykh, T.V., Fradkov, A.F., Ermakova, G.V., Solovieva, E.A., Lukyanov, K.A., Bogdanova, E.A., Zaraisky, A.G., Lukyanov, S., Chudakov, D.M., 2007. Bright far-red fluorescent protein for whole-body imaging. Nat. Methods 4, 741–746.

Stepanenko, O.V., Verkhusha, V.V., Shavlovskii, M.M., Aleinikova, T.D., Uverskii, V.N., Kuznetsova, I.M., Turoverov, K.K., 2005. The role of quarternary structure in fluorescent protein stability. Tsitologiia 47, 1017–1027.

Studier, F.W., 1991. Use of bacteriophage T7 lysozyme to improve an inducible T7 expression system. J. Mol. Biol. 219, 37–44.

Troise, F., Cafaro, V., Giancola, C., D'Alessio, G., De Lorenzo, C., 2008. Differential binding of human immunoagents and Herceptin to the ErbB2 receptor. FEBS J. 275, 4967–4979.

Tsien, R.Y., 2009. Constructing and exploiting the fluorescent protein paintbox (Nobel lecture). Angew. Chem. Int. Ed Engl. 48, 5612–5626.

Winter, G., 1998. Synthetic human antibodies and a strategy for protein engineering. FEBS Lett. 430, 92–94.

Winter, G., Milstein, C., 1991. Man-made antibodies. Nature 349, 293–299.

Worn, A., Pluckthun, A., 1998. An intrinsically stable antibody scFv fragment can tolerate the loss of both disulfide bonds and fold correctly. FEBS Lett. 427, 357–361.

Worn, A., Pluckthun, A., 2001. Stability engineering of antibody single-chain Fv fragments. J. Mol. Biol. 305, 989–1010.

Yang, F., Moss, L.G., Phillips Jr., G.N., 1996. The molecular structure of green fluorescent protein. Nat. Biotechnol. 14, 1246–1251.